Diagnostic classification of flash drought events reveals distinct classes of forcings and impacts

Mahmoud Osman[1,2], Benjamin F. Zaitchik[1], Hamada S. Badr[3], Jason Otkin[4], Yafang Zhong[4], David Lorenz[4], Martha Anderson[5], Trevor F. Keenan[6,7], David L. Miller[6], Christopher Hain[8], Thomas Holmes[9]

[1] *Department of Earth and Planetary Sciences, Johns Hopkins University, Baltimore, MD, USA.*

[2] *Irrigation and Hydraulics Department, Cairo University, Cairo, Egypt.*

[3] *Department of Civil and Systems Engineering, Johns Hopkins University, Baltimore, MD, USA.*

[4] *Space Science and Engineering Center, Cooperative Institute for Meteorological Satellite Studies, University of Wisconsin–Madison, WI, USA.*

[5] *Hydrology and Remote Sensing Laboratory, Agricultural Research Service, USDA, MD, USA.*

[6] *Department of Environmental Science, Policy, and Management, University of California, Berkeley, CA, USA.*

[7] *Earth and Environmental Sciences Area, Lawrence Berkeley National Lab., Berkeley, CA, USA.*

[8] *Earth Science Office, NASA Marshall Space Flight Center, Huntsville, AL, USA.*

[9] *Hydrological Sciences Laboratory, NASA Goddard Space Flight Center, Greenbelt, MD, USA.*

Corresponding author: Mahmoud Osman, mahmoud.osman@jhu.com; mahosman01@gmail.com

Abstract:

Recent years have seen growing appreciation that rapidly intensifying "flash droughts" are significant climate hazards with major economic and ecological impacts. This has motivated efforts to inventory, monitor, and forecast flash drought events. Here we consider the question of whether the term "flash drought" comprises multiple distinct classes of event, which would imply that understanding and forecasting flash droughts might require more than one framework. To do this, we first extend and evaluate a soil moisture volatility-based flash drought definition that we introduced in previous work and use it to inventory the onset dates and severity of flash droughts across the Contiguous United States (CONUS) for the period 1979-2018. Using this inventory, we examine meteorological and land surface conditions associated with flash drought onset and recovery. These same meteorological and land surface conditions are then used to classify the flash droughts based on precursor conditions that may represent predictable drivers of the event. We find that distinct classes of flash drought can be diagnosed in the event inventory. Specifically, we describe three classes of flash drought: "dry and demanding" events for which antecedent evaporative demand is high and soil moisture is low, "evaporative" events with more modest antecedent evaporative demand and soil moisture anomalies, but positive antecedent evaporative anomalies, and "stealth" flash droughts, which are different from the other two classes in that precursor meteorological anomalies are modest relative to the other classes. The three classes exhibit somewhat different geographic and seasonal distributions. We conclude that soil moisture "flash droughts" are indeed a composite of distinct types of rapidly intensifying droughts, and that flash drought analyses and forecasts would benefit from approaches that recognize the existence of multiple phenomenological pathways.

Introduction:

In recent years, a number of rapid-onset drought events have struck the Contiguous United States (CONUS), with severe consequences for ecological and agricultural systems. For example, droughts in the Southern Plains in 2011, the central U.S. in 2012, the Southeast in 2016, the Northern Plains in 2017, and Texas in 2019 led to widespread crop losses, wildfires, and economic damages in the tens of billions of dollars. These droughts occurred at different times of the year in different climate zones with different ecological characteristics, yet they have all been described as flash droughts, a term first coined by Peters et al. (2002) and Svoboda et al. (2002) to reflect the fact that some droughts emerge rapidly and quickly develop into high impact extreme events.

A challenging characteristic of flash droughts is that they appear suddenly—seemingly without warning—and therefore leave farmers, ranchers, and other vulnerable stakeholders little time to prepare mitigation responses (Otkin et al. 2015b, 2018a; Haigh et al. 2019). The 2012 flash drought, for example, received tremendous attention because of its impact on the nation's corn crop. Yet there was virtually no sign of an impending rapid intensification prior to the event in standard drought monitoring products at that time or in dynamically-based seasonal forecasting systems (Hoerling et al. 2014). Post-event analyses concluded that the event was largely driven by random atmospheric variability, and perhaps was inherently unpredictable using conventional methods (Kumar et al. 2013). Poor model performance both in forecasting and reproducing these events presents an additional challenge in efforts to project flash drought impacts and feedbacks under nonstationary climate conditions (Wolf et al. 2016). Notwithstanding these challenges, there is evidence that flash droughts are amenable to seasonal-to-subseasonal scale prediction on account of their sensitivity to initial conditions (Lorenz et al. 2017a,b), the perceived importance of forecastable drivers of evaporative demand during flash drought intensification (Hobbins et al.

2016), and the potentially predictable role of vegetation in flash drought processes (Wolf et al. 2016).

Any such generalized statements on the predictability of flash droughts, however, implicitly assume that the occurrence and severity of flash droughts can be diagnosed in a consistent and process-relevant manner, and that the term "flash drought" refers to a single class of event. In recent years, many studies have sought to describe and diagnose the occurrence of flash droughts by proposing a variety of definitions that can be used to inventory and map flash droughts. Otkin et al. (2013, 2014, 2015) identified flash droughts based on rapid changes in the ratio between actual evapotranspiration (EVP) and potential evapotranspiration (PEVP). Other studies (Hunt et al. 2014; Mo and Lettenmaier 2015) defined flash droughts as a function of the rapid drop in soil moisture with time. Chen et al. (2019) suggested the degradation of two categories in the U.S. Drought Monitor (USDM) in a period of four weeks as a definition for the onset of flash droughts. Christian et al. (2019) introduced the definition for flash droughts based on the rate of change in standardized ratio between EVP and PEVP over a six-pentad (6 x 5-day) period. Another quantitative definition (Ford and Labosier 2017) identified flash droughts as the drop of the one pentad averaged soil moisture (SM) from the 40^{th} to 20^{th} percentiles in a period of four pentads or less. A subsequent study by Hoffmann et al. (2021) followed a similar methodology with adjustments to reduce the number of identified events. In a recent study, (Osman et al. 2021) introduced a definition based on a soil moisture volatility index (SMVI), and also compared the SMVI with six other definitions to highlight the fact that there are different pathways to identify flash drought onset. All of the listed studies focused on CONUS, but the flash drought phenomenon has been observed in many regions across the globe (Nguyen et al. 2019; Zhang and Yuan 2020), with a number of studies focusing on China and India (Wang et al. 2016; Yuan et al. 2019; Mahto

and Mishra 2020). These studies have yielded additional definitions. Indeed, the need to understand the implications of different definitions has become a research question in its own right (Lisonbee et al. 2021).

Fewer studies have attempted to quantify the severity of the flash droughts, but informative efforts do exist. Chen et al. (2019) and Otkin et al. (2015) both used USDM categories to diagnose and assess severity of flash droughts. Christian et al. (2019) used Standardized Evaporative Stress Ratio (SESR) for both purposes, Yuan et al. (2019) used soil moisture deficit, and Li et al. (2020) used evapotranspiration deficit. Based on modeled soil moisture, Otkin et al. (2021) developed a flash drought intensity index (FDII) that explicitly accounts both for the magnitude of the rapid intensification and the resultant drought severity when determining the intensity of a flash drought. Their study showed that there are important regional differences in flash drought severity when both of these components are considered.

Most proposed definitions and intensity metrics for flash droughts have focused exclusively on capturing the phenomenon rather than assessing whether it represents a coherent class from the perspective of drought process. An exception is the work of Mo & Lettenmaier (2015, 2016), which explicitly distinguished between precipitation deficit flash droughts and heat wave flash droughts. The method used to define these droughts has been debated, in large part because Mo & Lettenmaier consider duration of the heatwave event rather than intensification rate, which is more typically understood to be the defining characteristic of flash drought (Otkin et al. 2018b; Lisonbee et al. 2021), but their concept that flash droughts might be the product of multiple different pathways with distinct meteorological drivers is highly relevant to understanding and prediction. While Mo & Lettenmaier made this distinction a priori by incorporating different variables and thresholds in their definitions, we are not aware of any study that empirically classifies different

92 flash drought types within an inventory generated using a common flash drought definition. That
93 is: if an inventory of flash drought events is generated using a definition based on flash drought
94 phenomenology alone, are there distinct classes within that inventory that can be identified due to
95 different precursors in meteorology or surface conditions? If so, that implies that understanding
96 and predicting flash droughts may require that we adopt different perspectives for each class.

97 Here, we apply our recently introduced SMVI flash drought definition (Osman et al. 2021) to
98 address this question. First, we extend the SMVI presented in Osman et al. (2021) to include
99 estimates of drought severity, and we compare the SMVI to independent vegetation and crop
100 datasets for seminal flash drought events. Next, we apply a retrospective inventory of flash
101 droughts, generated using SMVI, to derive composites of meteorological and surface conditions
102 in the pre-drought, onset, and recovery phases of all flash droughts. Finally, we perform objective
103 classification of the flash drought inventory on the basis of meteorological and surface condition
104 precursors to identify flash drought classes relevant to process understanding and prediction.

105 **Data and Methods:**

106 We generate an inventory of soil moisture flash droughts for all of CONUS over the period 1979-
107 2018 for spring through fall (March-November). SMVI is calculated using root zone soil moisture
108 (RZSM) from the SMERGE dataset. SMERGE is a hybrid daily product at 0.125° spatial
109 resolution that combines satellite-derived soil moisture estimates from the European Space Agency
110 Climate Change Initiative and NLDAS-2 NOAH model output for RZSM averaged from 0-40 cm
111 depth (Tobin et al. 2019). The SMERGE dataset has been evaluated against Normalized Difference
112 Vegetation Index (NDVI) products (Rouse et al. 1974) as well as in situ soil moisture observations,

and it has been found to be a reliable dataset for agricultural and ecological applications (Tobin et al. 2019).

The SMVI is motivated by the fact that flash drought diagnosis is concerned with capturing change that is more rapid than usual, so that it could be used to identify both rapid onset and rapid intensification drought events. For SMVI, rapid changes are identified by the crossover of simple moving averages (SMA's) combined with duration and dryness thresholds. Onset is recorded when: (1) The 5-day (1-pentad) RZSM SMA falls and stays below the 20-day (4-pentad) SMA for at least a 20-day period; (2) both SMA's are below the 20th percentile of the 1979 to 2018 time-of-year RZSM climatology (Osman et al. 2021). If two sequential flash droughts are identified with a period of three pentads or less between them, then they are combined into a single event. We do this because a short rainfall event may result in a temporary reduction in the severity of a flash drought but is often not sufficient to restore pre-drought conditions and end the drought event.

Severity is quantified based on RZSM deficit during the identified flash drought event according to Eq. 1 and Eq. 2 as illustrated in the example in Fig. S1. This scale is based on the standardized distribution of the integrated RZSM deficit below the 20th percentile (and over the 5-day running average) during the drought event.

$$SV = \sum_{t=t_o}^{t=t_f} (RZSM_{20th} - RZSM_{5d}) \qquad \text{Equation 1}$$

$$SV_{CAT} = \frac{SV}{STD(SV_{1979-2018})} \qquad \text{Equation 2}$$

where SV is the computed severity, and $RZSM_{20th}$ and $RZSM_{5d}$ are the 20th percentile and 5-day moving average RZSM, respectively. t_o and t_f represent the times at which identified flash drought onset occurs and ends, respectively. The standardized severity category is represented by

134 SV_{CAT} with a range between zero (no flash drought) up to 5 (maximum severity), and
135 $STD(SV_{1979-2018})$ is the severity standard deviation calculated from the flash drought inventory
136 for all grid points, measured against the severity of all other identified flash drought events within
137 the inventory. The use of categories to indicate drought severity is a common approach, as used in
138 systems such as the USDM. In contrast to the USDM, the SMVI-based severity is intended to
139 capture the severity of the rapid onset flash drought process.

140 The end of the flash drought period (recovery period) date is identified when the rate of drop in
141 RZSM during an identified flash drought event begins to recover (i.e., the 1-pentad running
142 average is no longer below 4-pentad running average) or the 1-pentad RZSM is no longer below
143 the 20th percentile of the 1979 to 2018 time-of-year RZSM.

144 SMVI performance was previously evaluated based on descriptions of reported major flash
145 drought events (Osman et al. 2021). Influenced by the methodology followed by Peters et al.
146 (2002) to detect drought using standardized NDVI, in this study we use MODIS NDVI time-of-
147 year anomalies to assess the method's skill to capture changes in satellite-observed vegetation
148 greenness due to flash drought. The cloud-free NDVI data were obtained from the 16-day MODIS
149 composite product (MOD13C1) at 0.05° spatial resolution (Didan 2021) for the years 2000 to
150 present. NDVI grid points with anomalies below -0.5 standard deviation from the mean are defined
151 as "negatively impacted" in comparisons with SMVI. This approximately corresponds to a
152 probability of occurrence less than 30% for normally distributed conditions. Further, we evaluate
153 the performance of the SMVI definition for the 2012 central US and 2017 Northern Plains flash
154 droughts versus in situ reports of soil and crop conditions collected by the USDA National
155 Agricultural Statistics Service (NASS) observers. Data showing poor conditions are marked as
156 negatively impacted. These data are collected at county scale, then spatially smoothed to reduce

157 noise, and protect confidentiality (Access to data at county level was provided to the co-authors
158 after signing a confidentiality agreement with the USDA NASS). The performance analyses are
159 carried out for the spring and summer seasonal averages due to data availability and temporal
160 resolution.

161 The performance of the SMVI is assessed with hit-miss confusion matrices that use NDVI and
162 NASS data as observational reference datasets. True positive values represent grid points and
163 pentads depicted by SMVI as being in flash drought and also marked as negatively impacted by
164 the NASS or NDVI validation datasets, while false positives are the events classified as flash
165 drought by SMVI where NASS or NDVI do not meet drought impact criteria. True negative values
166 represent grid points not marked as negatively impacted by the NASS or NDVI validation datasets
167 and not identified as flash drought grid points. False negatives represent grid points identified by
168 SMVI as having no flash drought while marked as negatively impacted by the NASS or NDVI
169 validation datasets. Hit-miss statistics are calculated according to Eq. 3 to Eq. 10.

170 $$Sensitivity\ (TPR) = \frac{TP}{TP+FN}$$ Equation 3

171 $$Specificity\ (TNR) = \frac{TN}{TN+FP}$$ Equation 4

172 $$False\ discovery\ rate\ (FDR) = \frac{FP}{FP+TP}$$ Equation 5

173 $$False\ Negative\ Rate\ (FNR) = \frac{FN}{FN+TP}$$ Equation 6

174 $$False\ Positive\ Rate\ (FPR) = \frac{FP}{FP+TN}$$ Equation 7

175 $$Precision\ (PPV) = \frac{TP}{TP+FP}$$ Equation 8

$$Accuracy\ (ACC) = \frac{TP+TN}{TP+TN+FP+FN} \quad \text{Equation 9}$$

$$Critical\ Success\ Index\ (CSI) = \frac{TP}{TP+FN+FP} \quad \text{Equation 10}$$

where, $TP, TN, FP\ and\ FN$ represent true positive, true negative, false positive and false negative grid points, respectively. Values of Eq. 3 to Eq. 10 range from 0 to 1, with 1 being the perfect score for the TP or TN numerator-based ratios and the opposite for the FP and FN numerator-based ratios.

Drawing on previous studies that have described meteorological and surface conditions associated with flash drought onset (Mo and Lettenmaier 2015, 2016; Ford and Labosier 2017; He et al. 2019; Osman et al. 2021), we select multiple variables from the NLDAS-2 datasets (temperature, precipitation, RZSM, PEVP, EVP, and surface pressure) along with the computed vapor pressure deficit (VPD) and total cloud cover (TCC) from NCEP/NCAR Reanalysis Products (Kalnay et al. 1996), and analyze their progression through the pre-drought, onset and end of the flash drought periods for all events included in the 40-year (1979-2018) SMVI-derived flash drought inventory. In order to focus on events with meaningful impact, we analyze only SMVI-derived flash drought events with severity greater than 2. Unsupervised multivariate classification is then performed as a function of these meteorological variables, using principal components transformation to control for collinearity between variables. This classification is used to characterize different types of flash droughts driven by different processes. The classes are determined using the K-means partitioning unsupervised classification algorithm (Hartigan and Wong 1979; Lloyd 1982) as a heuristic clustering method. We apply a sensitivity analysis to determine the statistically optimal number of clusters. The anomalies are calculated as the in-time (pre-drought, onset, or recovery) pentad anomaly relative to the 1979-2018 time-of-year average. The K-means algorithm allows the user

198 to set the number of classes subjectively, but there are recommended diagnostics for use in
199 choosing the optimal number of classes. Here we apply the commonly-used Elbow method
200 (Thorndike 1953) for this purpose.

201 **Results and Discussion:**

202 *The SMVI flash drought intensity metric*

203 The United States was hit by several major flash drought events over the past decade, resulting in
204 excessive agricultural losses and livestock destruction. In 2012, the country experienced one of the
205 largest and most destructive flash droughts recorded to date, with more than $30 billion estimated
206 damages (Hoerling et al. 2013, 2014; Basara et al. 2019; Mallya et al. 2013; Fuchs et al. 2012;
207 Otkin et al. 2016). A warm spring followed by early summer heatwaves set the stage for a rapidly
208 intensifying drought that struck much of the middle part of the country in late spring and early
209 summer and extended to the north later in summer and in early fall (Fig. 1a). Notably, though the
210 occurrence of flash drought was very widespread (according to both SMVI and other definitions)
211 (Osman et al. 2021), the central US had the greatest severity, as diagnosed by the SMVI (Fig, 1c).

212 Five years after the 2012 flash drought, the Northern Plains region was hit by another major flash
213 drought, causing more than $2.6 billion agricultural losses, and sparking wildfires. The 2017
214 Northern Plains flash drought was focused on Montana, North Dakota, South Dakota, and parts of
215 Alberta and Saskatchewan (Jencso et al. 2019). The event started in May over western Montana
216 and swiftly intensified through high evaporative demand and precipitation deficits (Hoell et al.
217 2019a; Osman et al. 2021). The drought eventually spread over much of the Northern Plains region
218 (Fig. 1b) causing enormous economic losses (Gerken et al. 2018; Jencso et al. 2019; He et al.
219 2019). Montana was the most impacted state (Jencso et al. 2019), and this is evident in the SMVI-

based severity analysis (Fig. 1d). The severity analysis is also consistent with the USDM reports that showed an exceptional (D4 category) drought over Montana (Jencso et al. 2019). It is important to highlight that estimation of flash droughts' severity in this study is a method to relatively quantify soil moisture deficit with a methodology similar to Yuan et al. (2019) study given the different flash drought identification method.

Independent, quantitative validation of drought indices is notoriously difficult, since impacts of drought vary with climate context, land cover, and economic system. Since flash drought is a subset of all droughts which is typically considered in agricultural and ecological contexts (Wang et al. 2016; Mo and Lettenmaier 2015; Christian et al. 2019; Otkin et al. 2018b), we consider vegetation health and crop status to be two relevant indicators of drought impact that can verify the utility of SMVI as a useful drought metric. In doing this, we recognize that the independent comparisons do not necessarily confirm the presence of flash drought; rather, they are interpreted as indicators of whether an agricultural drought may have occurred.

With this caveat in mind, we compare the SMVI flash drought index to MODIS NDVI anomalies and NASS crop and topsoil condition anomalies. Using a simple hit/miss metric in which negative anomalies in MODIS NDVI (more than 0.5 standard deviation below the mean) or the NASS condition maps are interpreted as evidence of drought conditions, we find that there is broad agreement between the SMVI and observed drought conditions for both the 2012 and 2017 flash drought events (Fig. 1 and Fig. 2). We do see considerable false negatives on the margins of the drought-affected area, particularly in 2012, but this is consistent with our liberal definition of agricultural drought in the NDVI and NASS fields (i.e., flash drought identified area is smaller than NDVI and NASS negative anomalies). We also note a concentration of false positives along

edge of drought regions, particularly in 2017, indicate that the SMVI approach overestimated the extent of drought-affected area relative to NASS estimates.

Focusing on the Central and Northern High Plains regions (as defined by Bukovsky (2011)) for the years 2012 and 2017, respectively, we find that for flash droughts based on negative NDVI anomalies the accuracy was 0.68 in 2012 and 0.56 in 2017. Precision was higher in 2012 (0.74) than 2017 (0.50), while the probability of detection (sensitivity) was higher in 2017: 0.93, versus 0.81 in 2012 (Tables 1&2). The Critical Success Index was significantly higher for the 2012 event (0.63) compared to that observed in 2017 (0.48). These values of hit-miss statistics are consistent with moderate to strong performance in event identification (Hoerling et al. 2013, 2014; Basara et al. 2019; Mallya et al. 2013; Fuchs et al. 2012; Otkin et al. 2016; Gerken et al. 2018; Jencso et al. 2019; He et al. 2019). It is important to note that this is an imperfect comparison. The SMVI approach is one pathway of identifying flash droughts, and a comparison with a vegetation index metric, such as NDVI anomalies, is not exactly indicative of performance in capturing a soil moisture flash drought.

NASS-based evaluation, based on NASS identification of poor crop and soil conditions, led to comparable statistics for each impacted region's dominant crop (Fig. 2c – 2f). Tables 1 and 2 summarize SMVI-NASS statistics for both the 2012 and 2017 flash droughts. In the 2012 central US flash drought, SMVI shows an accuracy of 0.79, 0.75 and 0.74 for negatively impacted soybean, range, and corn, with a precision of 0.84, 0.79 and 0.89, respectively. The 2017 Northern Plains flash drought captured by SMVI is similarly evaluated and statistical evaluation was slightly higher than that seen for the NDVI analysis. Accuracy for detecting grids of flash drought in the Northern Plains compared to negatively impacted dominant crops (barley and spring wheat) are 0.8 and 0.76, respectively, with precision values of 0.91 and 0.88, and probability of detection

greater than 0.84. Comparing SMVI to the reported NASS topsoil moisture conditions shows a very similar pattern for the negatively reported conditions. The accuracy and precision of SMVI detection of the reported negative NASS topsoil moisture conditions for the 2012 flash drought event are 0.77 and 0.95, respectively, and they are 0.84 and 0.95 for the 2017 event. We also note that irrigation is a complicating factor that may affect comparison between datasets. While SMVI does include partial consideration of irrigation, insomuch as SMERGE captures irrigation signals, this representation is imperfect and might not align with observed vegetation response to irrigation.

Proposed drivers of flash drought:

Figure 3 presents composites of pre-drought (onset minus three pentads), onset, and recovery period conditions, using composites of standardized anomalies of meteorological fields for all flash droughts of severity greater than '2' in the SMVI-derived 1979-2018 inventory. Composites are calculated separately for each grid cell, such that the anomalies represent conditions when a flash drought occurred in that exact location. Precipitation (PRCP) anomalies in the pre-drought and onset periods are mostly negative, as one would expect, which is also associated with suppression of the convective available potential energy (CAPE) over most of CONUS (we include CAPE in addition to precipitation in order to isolate local convective potential as distinct from total realized rainfall). This is similar to the observed scenario before and during the 2017 northern High Plains flash drought (Gerken et al. 2018). The magnitude of these standardized anomalies, however, is generally small relative to the anomalies in RZSM and potential evaporation (PEVP), particularly during the pentad of drought onset.

These findings are consistent with previous studies (Otkin et al. 2018b, 2013; Anderson et al. 2013), which have emphasized the importance of precursor soil moisture conditions and PEVP in

the onset of a flash drought. Low RZSM, high PEVP and high VPD conditions force the rapid transition from an energy limited environment to a water limited environment, leading to rapid drought onset and loss of green cover (Otkin et al. 2018b). This elevated PEVP only leads to an increase in actual evapotranspiration (EVP) in regions with greater water variability—e.g., the Midwest and Great Lakes regions. In more water limited environments the EVP anomalies are negative in the pre-drought and onset periods, as elevated PEVP cannot translate into an increase in EVP. As described later, this distinction is important when considering process-based flash drought classification: the concept that elevated PEVP leads to elevated EVP, drying the soil column, is an important aspect of some theories of vegetation-mediated flash drought intensification (Otkin et al. 2018b), but it is not a feature of all events in our inventory.

Other potential predictor variables show regionally variable signals. Temperature (TEMP), often identified as a driver of flash drought, is generally elevated in the pre-drought period, but the anomalies are weak, and the sign of anomaly is not entirely consistent. It is only during the onset pentad that elevated temperatures are observed over most regions (though even then the southeast is not particularly anomalously warm). Surface pressure (SPRES) might be expected to be anomalously high in the lead-up to a drought, but the anomalies are weak and mixed over much of the country, as is the average near-surface wind speed (WS). TCC tends towards negative anomalies in pre-drought and onset periods, matching expectation, but again there are weak or mixed anomalies for a number of regions.

Considering the recovery pentad, which is defined as the first pentad in which any of the onset conditions is violated, it is evident that the role of rainfall is significant in ending the flash drought. Both PRCP and TCC show strong positive anomalies in recovery, which stands in contrast to the modest anomalies seen during the pre-drought and onset periods. Rain breaks the flash drought

cycle, quickly switching environmental conditions to a non-water-limited status, provided that the volume of rain is sufficient. TEMP, PEVP, EVP, VPD and SPRES anomalies are mixed during the recovery period. RZSM anomalies are still strongly negative, reflecting the fact that we have defined the recovery (end of flash drought period) based on the change in rate of declination or if RZSM higher than the 20^{th} percentile, which are still below normal conditions but no longer a flash drought. It is worth emphasizing that these composites are based on our SMVI flash drought definition; analyses that use different definitions might lead to different conclusions. That said, Ford and Labosier (2017) examine some of the same variables and found broadly similar patterns using a different flash drought definition formulation based on the drop in RZSM from the 40^{th} to the 20^{th} percentile in a period that does not exceed four pentads.

Flash drought classification

The composite analysis of conditions at different stages of flash droughts shown in the previous section provides a useful perspective on the flash drought development process; however, it does not consider the possibility that the inventoried flash droughts consist of distinct forms of drought development. It is therefore possible that the weak or mixed anomalies found for certain proposed drivers are simply an artifact of averaging across different types of events, blurring the influence of hydrometeorological drivers in different drying scenarios.

To test this hypothesis, we perform K-means classification on our SMVI based flash drought inventory. We use onset pentad standardized anomalies for the nine variables applied in composite analysis (TMP, PRCP, RZSM, EVP, PEVP, SPRES, TCC, WS, CAPE and VPD) as the basis for classification, and first mask out unvegetated classes (bare soil and urban classes) and potentially deep-rooted vegetation classes (forest and woodland classes) according to the University of

Maryland (UMD) Land Cover Classification (Figure S2). Only events with severity greater than '2' are included in the classification, and we perform principle components analysis on meteorological variables prior to classification. Using the Elbow method (Thorndike 1953), we find that three classes are optimal (Figure S3). We emphasize that our classification is intended to draw out indicative patterns and is not meant to imply that the three classes are entirely separable or independent phenomena. The use of a different dataset of meteorological variables, study region, or flash droughts identification method may lead to a different number of classes.

The character of each class with respect to precursor soil moisture conditions and meteorology in the pentads leading up to event onset is shown in Figure 4. Notably, Classes 2 and 3 are characterized by elevated air temperature (TMP) and vapor pressure deficit (VPD) prior to flash drought onset, while Class 1 is not. And while Class 2 and 3 have similar TMP anomalies, Class 2 exhibits substantially more severe antecedent VPD than Class 3, as well as stronger positive potential evapotranspiration (PEVP) anomalies and stronger negative root zone soil moisture (RZSM) and total cloud cover (TCC) anomalies. Class 3, meanwhile, is the only class that shows positive anomalies in antecedent actual evapotranspiration (EVP) and in CAPE, and its negative precipitation (PRCP) anomalies are modest relative to the other two classes.

These systematic differences between classes suggests that flash droughts can be triggered by a diversity of meteorological conditions. Class 2 bears the most classic signatures of drought, with its dry antecedent conditions, high temperature and evaporative demand conditions, low cloud cover, and reduced total evapotranspiration. From a flash drought perspective, these can be thought of as "dry and demanding" events, in which atmospheric evaporative demand combines with low rainfall and dry pre-drought conditions to allow for rapid intensification of already dry conditions. Notably, PEVP anomalies for these events tend to be quite high, but EVP anomalies are strongly

355 negative on account of the prevailing dry conditions prior to drought onset. It is important to
356 emphasize that our interpretation of the different classes is based on the mean value, which adds a
357 margin of uncertainty in classifying an identified flash drought event. Figure 5b shows composite
358 time series of key variables for 20 grid cells picked from the core of different Class 2 drought
359 events. As indicated in these time series, TMP, VPD, and PEVP are all elevated in the four pentads
360 before flash drought onset while EVP anomalies are consistently negative over this period. PRCP
361 anomalies are generally negative, with some noise evident in this 20 grid cell sample, while NDVI
362 and RZSM anomalies are strongly negative even four pentads before onset date.

363 In contrast to the classic drought character of Class 2, Class 3 bears some surprising features. The
364 fact that the events intensify rapidly even though, on average, the antecedent PRCP anomalies are
365 modest and CAPE is enhanced, suggest that for these events rapid drying is largely driven by
366 evaporative demand (positive VPD and PEVP anomalies) combined with sufficient moisture
367 access to support elevated EVP. This combination makes Class 3 the only class to exhibit
368 anomalies consistent with the hypothesis that vegetation can contribute to flash drought onset by
369 responding to elevated temperature and evaporative demand with increased evapotranspiration,
370 accelerating depletion of root zone soil moisture. Based on these characteristics, we term Class 3
371 events “evaporative” flash droughts. As shown in Figure 5c for a random sample of points from
372 different Class 3 events, PRCP anomalies are mixed, with a negative signal only evident in the 2
373 pentads before onset, and positive anomalies seen at longer leads and even after flash drought
374 onset. EVP is consistently elevated before and during onset, while strongly positive TMP, VPD,
375 and PEVP anomalies emerge only in the two pentads before onset. Interestingly, RZSM and NDVI
376 anomalies are, on average for this sample, positive until two pentads before onset, such that the

377 rapid decline observed just before onset leads to negative anomalies that are substantially smaller
378 than those observed for Class 2 events at date of onset.

379 Class 1, for its part, is noteworthy for the fact that air temperature and evaporative demand
380 preceding flash drought onset are unremarkable compared to average conditions. Precipitation is
381 below average in the pre-drought period, skies are relatively clear (low TCC), and convective
382 potential is low (negative CAPE anomaly). But anomalies in all other variables commonly invoked
383 to explain the rapidity of flash drought intensification are modest, i.e., there is a near-zero
384 temperature, PEVP and VPD pre-drought anomalies. In this sense, Class 1 flash droughts appear
385 to be dominated by precipitation deficit forcing rather than evaporative demand forcing, placing
386 them at a far end of the PEVP vs. PRCP balance of flash drought forcings described by Christian
387 et al. (2021). As described later, Class 1 events are, on average, slightly less severe than other
388 classes, but they are not always low severity events. We will refer to these events as "stealth" flash
389 droughts in that they have characteristics that would make them difficult to forecast: where Classes
390 2 and 3 show meteorological drivers that might be forecasted with skill at extended weather to
391 subseasonal timescales, Class 1 appears to be the product almost solely of moderately dry
392 antecedent soil moisture and below average rainfall, which can be difficult to predict with precision
393 more than a few days in advance (Tian et al. 2017). The sample timeseries shown in Figure 5a
394 indicates that positive anomalies in VPD and PEVP are modest and emerge only within two
395 pentads of onset, and TMP anomalies are essentially neutral. Interestingly, the decline in NDVI is
396 dramatic for this class, suggesting that these events strike vegetation that is particularly sensitive
397 to drought stress on account of vegetation type or timing. The fact that NDVI anomalies are
398 strongly positive at three and four pentad leads, and that negative EVP signals are not evident at

399 longer leads, suggests that these events might be associated with favorable early season growing
400 conditions leading to structural overshoot in vegetation (Zhang et al., 2021).

401 At the national scale, 45% of all flash drought events in our inventory are Class 1, 31% are Class
402 2, and 22% are Class 3. But there are distinct geographic patterns for each (Figure 6). Class 1
403 events are most common in the western High Plains, Class 2 are dominant in the Southern Great
404 Plains and Texas, and Class 3 are the most common type in the upper Midwest. This is not a
405 deterministic split—all three classes are found in all regions—but the geographic distribution
406 aligns with expectation. In the relatively humid and cool upper Midwest, one might expect that
407 high TMP and VPD can trigger elevated EVP even when soils are somewhat dry relative to their
408 average state, while in the warmer and drier Southern Great Plains those conditions are less likely
409 to be met with increased EVP: conditions are simply too dry. The prevalence of Class 1 events in
410 the western High Plains is less easily explained, but it is consistent with experience in that the
411 iconic 2017 flash drought that affected Montana and North Dakota was a notably poorly predicted
412 event (Jencso et al. 2019; Hoell et al. 2019b) .

413 Indeed, if we map the class associations of the 2017 flash drought event, along with the seminal
414 flash drought events of 2011 and 2012 (Figure 7), we see that 2017 was almost entirely Class 1.
415 The 2011 event, focused on Texas and Oklahoma, is predominantly Class 2. The widespread event
416 of 2012 is a mix of Class 2 and Class 3, consistent with the fact that this was a hot event affecting
417 a broad swath of the Great Plains and Midwest, including a diversity of climate zones and land
418 cover types.

419 Seasonally, all three flash drought classes can be observed in any month included in our analysis
420 (March-November; Figure 8). Class 2 shows a dramatic peak in June, coincident with the onset of
421 summer heat and dryness over much of the drought-susceptible United States. Class 3 shows a

similar, albeit more muted June peak. This is the least common flash drought class on average, but in the spring it does show slightly greater total area than Class 2, and the drop in area after June is dramatic. This is consistent with a drought process that includes sufficient available soil moisture to support elevated EVP. Class 1, meanwhile, is the most widespread drought class in all months except for June, when it is briefly exceeded by Class 2. The fact that Class 1 events continue to be relatively common in late summer is in part a reflection of geography, since these events dominate in some of the coolest portions of the analysis domain. The drivers of flash drought risk, then, appear to vary by both region and season, a fact that is relevant for the development of flash drought risk monitoring and forecasting systems. We note that these seasonal patterns are sensitive to our inventory method, which is subject to the previously discussed assumptions, and clustering may vary accordingly. We note that our inventory method, which includes only the first instance of flash drought in each grid cell in each year, may slightly underrepresent late season flash droughts in general, since in cases of two flash droughts in the same location in the same year (which are rare) the second event would not be captured by our method.

Finally, we find that all three diagnosed classes of flash drought include cases of severe drought (according to our created inventory of flash droughts severity from Eq. 1 and Eq. 2), but that there are statistical differences in severity between classes, as estimated using the SMVI severity classes defined in this study (Figure 9). There is a slight tendency for greater severity in Class 2, the “dry and demanding” droughts, and the most severe events in the record are dominated by Class 2, followed by slightly decreased average severity for Class 3 and Class 1. The differences in severity between classes are statistically significant, as evaluated using a Welch t-test, for both raw and log transformed data, and confirmed with a non-parametric Wilcoxon signed-rank test. This result emphasizes the potential severity of flash droughts that develop under the combined conditions of

high evaporative demand, low precipitation, and dry antecedent conditions. Nevertheless, the distribution of event severities shown in Figure 9 makes it clear that all three classes contain severe events. This is also clear from our analysis of seminal flash droughts (Figure 1). We note that Figure 9 shows results for events filtered for severity greater than 2, but that the same general pattern is observed when we do not apply a severity threshold.

Conclusions:

Flash drought has proven to be a challenging phenomenon for both monitoring and prediction. These challenges have been associated with the rapidly evolving nature of the events and, perhaps, with the fact that they depend on processes that may not be explicitly resolved, or may be poorly predicted, in standard subseasonal to seasonal forecast systems. But terminology and definitions have also been challenging (Lisonbee et al. 2021), and the difficulty of establishing consistent and agreed-upon definitions is also a significant contributor to associated challenges in prediction. If the physical interpretation of a flash drought inventory is not sufficiently clear, then it is also not clear what one is predicting with a statistical model trained using that inventory, or what one is evaluating when considering a dynamically-based forecast of an event.

Here, we have examined meteorological drivers associated with events inventoried using an SMVI-based definition of flash drought events, and then classified all events in the inventory on the basis of precursor meteorological and surface conditions. We found three classes of flash droughts in our inventory based on K-means clustering. We refer to these classes as: "dry and demanding" droughts, with high evaporative demand and antecedent low soil moisture levels; "evaporative" droughts, which initiate under conditions of high demand and when elevated evapotranspiration accelerates soil drying; and "stealth" droughts, which may be hard to predict

due to the lack of a clear temperature or evaporative demand signal prior to initiation. These classes are associated with different meteorological variables, regional distributions, seasonality, and climatic and land surface risk factors, suggesting that there are distinct forms of flash drought development.

We emphasize that the classes defined here are representative of a continuum of processes associated with flash drought development. We choose to work with three classes because it proved to be a stable, separable, and interpretable number of classes in our analysis, but the result does not imply that there are only three pathways that can lead to flash drought, or that an event cannot exhibit a mix of properties from two or three classes. The contrasting meteorological and surface process signatures of the three classes do, however, indicate that events identified as "flash drought" using a reasonable definition, including events that have been widely reported as seminal flash droughts, represent a diversity of onset and intensification processes. Our results suggest that recognizing this diversity is critical to advance our understanding and ability to predict these events.

References

Anderson, M. C., C. Hain, J. Otkin, X. Zhan, K. Mo, M. Svoboda, B. Wardlow, and A. Pimstein, 2013: An Intercomparison of Drought Indicators Based on Thermal Remote Sensing and NLDAS-2 Simulations with U.S. Drought Monitor Classifications. *J. Hydrometeorol.*, **14**, 1035–1056, https://doi.org/10.1175/jhm-d-12-0140.1.

Basara, J. B., J. I. Christian, R. A. Wakefield, J. A. Otkin, E. H. Hunt, and D. P. Brown, 2019: The evolution, propagation, and spread of flash drought in the Central United States during 2012. *Environ. Res. Lett.*, **14**, https://doi.org/10.1088/1748-9326/ab2cc0.

489 Chen, L. G., J. Gottschalck, A. Hartman, D. Miskus, R. Tinker, and A. Artusa, 2019: Flash Drought
490 Characteristics Based on U.S. Drought Monitor. *Atmosphere (Basel).*, **10**, 498,
491 https://doi.org/10.3390/atmos10090498.

492 Christian, J. I., J. B. Basara, J. A. Otkin, E. D. Hunt, R. A. Wakefield, P. X. Flanagan, and X. Xiao,
493 2019: A Methodology for Flash Drought Identification: Application of Flash Drought
494 Frequency Across the United States. *J. Hydrometeorol.*, JHM-D-18-0198.1,
495 https://doi.org/10.1175/JHM-D-18-0198.1.

496 Didan, K., 2021: MODIS/Terra Vegetation Indices 16-Day L3 Global 0.05Deg CMG V061. *NASA*
497 *EOSDIS L. Process. DAAC*, https://doi.org/10.5067/MODIS/MOD13C1.061.

498 Ford, T. W., and C. F. Labosier, 2017: Meteorological conditions associated with the onset of flash
499 drought in the Eastern United States. *Agric. For. Meteorol.*, **247**, 414–423,
500 https://doi.org/10.1016/J.AGRFORMET.2017.08.031.

501 Fuchs, B., D. Wood, and D. Ebbeka, 2012: From Too Much to Too Little: How the Central US
502 Drought of 2012 Evolved Out of One of the Most Devastating Floods on Record in 2011.
503 *Natl. Integr. Drought Inf. Syst.*, 105.
504 https://www.drought.gov/drought/sites/drought.gov.drought/files/media/reports/regional_ou
505 tlooks/CentralRegion2012DroughtAssessment_1-5-15.pdf.

506 Gerken, T., G. T. Bromley, B. L. Ruddell, S. Williams, and P. C. Stoy, 2018: Convective
507 suppression before and during the United States Northern Great Plains flash drought of 2017.
508 **22**, 4155–4163, https://doi.org/10.5194/hess-22-4155-2018.

509 Haigh, T. R., J. A. Otkin, A. Mucia, M. Hayes, and M. E. Burbach, 2019: Drought Early Warning
510 and the Timing of Range Managers' Drought Response. *Adv. Meteorol.*, **2019**,

https://doi.org/10.1155/2019/9461513.

Hartigan, J. A., and M. A. Wong, 1979: A K-Means Clustering Algorithm. *Appl. Stat.*, **28**, 100, https://doi.org/10.2307/2346830.

He, M., J. S. Kimball, Y. Yi, S. Running, K. Guan, K. Jensco, B. Maxwell, and M. Maneta, 2019: Impacts of the 2017 flash drought in the US Northern plains informed by satellite-based evapotranspiration and solar-induced fluorescence. *Environ. Res. Lett.*, **14**, 074019, https://doi.org/10.1088/1748-9326/ab22c3.

Hobbins, M. T., A. Wood, D. J. McEvoy, J. L. Huntington, C. Morton, M. Anderson, and C. Hain, 2016: The Evaporative Demand Drought Index. Part I: Linking Drought Evolution to Variations in Evaporative Demand. *J. Hydrometeorol.*, **17**, 1745–1761, https://doi.org/10.1175/JHM-D-15-0121.1.

Hoell, A., and Coauthors, 2019a: Anthropogenic Contributions to the Intensity of the 2017 United States Northern Great Plains Drought. *Bull. Am. Meteorol. Soc.*, **100**, S19–S24, https://doi.org/10.1175/BAMS-D-18-0127.1.

——, J. Perlwitz, and J. Eischeid, 2019b: *The Causes, Predictability, and Historical Context of the 2017 U.S. Northern Great Plains Drought*. 25 pp. https://www.drought.gov/drought/sites/drought.gov.drought/files/2017-NGP-drought-assessment.pdf (Accessed June 11, 2019).

Hoerling, M., S. Schubert, and K. C. Mo, 2013: *An Interpretation of the Origins of the 2012 Central Great Plains Drought Assessment Report*. 50 pp.

Hoerling, M., J. Eischeid, A. Kumar, R. Leung, A. Mariotti, K. Mo, S. Schubert, and R. Seager,

2014: Causes and Predictability of the 2012 Great Plains Drought. *Bull. Am. Meteorol. Soc.*, **95**, 269–282, https://doi.org/10.1175/bams-d-13-00055.1.

Hoffmann, D., A. J. E. Gallant, and M. Hobbins, 2021: Flash drought in cmip5 models. *J. Hydrometeorol.*, **22**, 1439–1454, https://doi.org/10.1175/JHM-D-20-0262.1.

Hunt, E. D., M. Svoboda, B. Wardlow, K. Hubbard, M. Hayes, and T. Arkebauer, 2014: Monitoring the effects of rapid onset of drought on non-irrigated maize with agronomic data and climate-based drought indices. *Agric. For. Meteorol.*, **191**, 1–11, https://doi.org/10.1016/j.agrformet.2014.02.001.

Jencso, K., and Coauthors, 2019: *Flash drought: Lessons learned from the 2017 drought across the U.S. northern plains and Canadian prairies*. https://www.drought.gov/drought/sites/drought.gov.drought/files/NIDIS_LL_FlashDrought_2017_high-res_Final.pdf.

Kalnay, E., and Coauthors, 1996: The NCEP/NCAR 40-Year Reanalysis Project. *Bull. Am. Meteorol. Soc.*, **77**, 437–471, https://doi.org/10.1175/1520-0477(1996)077<0437:TNYRP>2.0.CO;2.

Kumar, A., M. Chen, M. Hoerling, and J. Eischeid, 2013: Do extreme climate events require extreme forcings? *Geophys. Res. Lett.*, **40**, 3440–3445, https://doi.org/10.1002/grl.50657.

Li, J., Z. Wang, X. Wu, J. Chen, S. Guo, and Z. Zhang, 2020: A new framework for tracking flash drought events in space and time. *Catena*, **194**, 104763, https://doi.org/10.1016/j.catena.2020.104763.

Lisonbee, J., M. Woloszyn, and M. Skumanich, 2021: Making sense of flash drought: definitions,

553 indicators, and where we go from here. *J. Appl. Serv. Climatol.*, **2021**, 1–19,
554 https://doi.org/10.46275/JOASC.2021.02.001.

555 Lloyd, S., 1982: Least squares quantization in PCM. *IEEE Trans. Inf. Theory*, **28**, 129–137,
556 https://doi.org/10.1109/TIT.1982.1056489.

557 Lorenz, D. J., J. A. Otkin, M. Svoboda, C. R. Hain, M. C. Anderson, and Y. Zhong, 2017a:
558 Predicting the U.S. Drought Monitor Using Precipitation, Soil Moisture, and
559 Evapotranspiration Anomalies. Part II: Intraseasonal Drought Intensification Forecasts. *J.*
560 *Hydrometeorol.*, **18**, 1963–1982, https://doi.org/10.1175/JHM-D-16-0067.1.

561 ——, ——, ——, ——, ——, and ——, 2017b: Predicting U.S. drought monitor states using
562 precipitation, soil moisture, and evapotranspiration anomalies. Part I: Development of a
563 nondiscrete USDM index. *J. Hydrometeorol.*, **18**, 1943–1962, https://doi.org/10.1175/JHM-
564 D-16-0066.1.

565 Mahto, S. S., and V. Mishra, 2020: Dominance of summer monsoon flash droughts in India.
566 *Environ. Res. Lett.*, https://doi.org/10.1088/1748-9326/abaf1d.

567 Mallya, G., L. Zhao, X. C. Song, D. Niyogi, and R. S. Govindaraju, 2013: 2012 Midwest drought
568 in the United States. *J. Hydrol. Eng.*, **18**, 737–745, https://doi.org/10.1061/(ASCE)HE.1943-
569 5584.0000786.

570 Mo, K. C., and D. P. Lettenmaier, 2015: Heat wave flash droughts in decline. *Geophys. Res. Lett.*,
571 **42**, 2823–2829, https://doi.org/10.1002/2015gl064018.

572 Mo, K. C., and D. P. Lettenmaier, 2016: Precipitation Deficit Flash Droughts over the United
573 States. *J. Hydrometeorol.*, **17**, 1169–1184, https://doi.org/10.1175/jhm-d-15-0158.1.

574 Nguyen, H., M. C. Wheeler, J. A. Otkin, T. Cowan, A. Frost, and R. Stone, 2019: Using the
575 evaporative stress index to monitor flash drought in Australia. *Environ. Res. Lett.*, **14**, 064016,
576 https://doi.org/10.1088/1748-9326/ab2103.

577 Osman, M., B. F. Zaitchik, H. S. Badr, J. I. Christian, T. Tadesse, J. A. Otkin, and M. C. Anderson,
578 2021: Flash drought onset over the contiguous United States: sensitivity of inventories and
579 trends to quantitative definitions. *Hydrol. Earth Syst. Sci.*, **25**, 565–581,
580 https://doi.org/10.5194/hess-25-565-2021.

581 Otkin, J. A., M. C. Anderson, C. Hain, I. E. Mladenova, J. B. Basara, and M. Svoboda, 2013:
582 Examining Rapid Onset Drought Development Using the Thermal Infrared–Based
583 Evaporative Stress Index. *J. Hydrometeorol.*, **14**, 1057–1074, https://doi.org/10.1175/JHM-
584 D-12-0144.1.

585 ——, ——, ——, M. Svoboda, J. A. Otkin, M. C. Anderson, C. Hain, and M. Svoboda, 2014:
586 Examining the Relationship between Drought Development and Rapid Changes in the
587 Evaporative Stress Index. *J. Hydrometeorol.*, **15**, 938–956, https://doi.org/10.1175/JHM-D-
588 13-0110.1.

589 ——, ——, ——, ——, ——, ——, ——, and ——, 2015a: Using Temporal Changes in Drought
590 Indices to Generate Probabilistic Drought Intensification Forecasts. *J. Hydrometeorol.*, **16**,
591 88–105, https://doi.org/10.1175/jhm-d-14-0064.1.

592 ——, M. Shafer, M. Svoboda, B. Wardlow, M. C. Anderson, C. Hain, and J. Basara, 2015b:
593 Facilitating the use of drought early warning information through interactions with
594 agricultural stakeholders. *Bull. Am. Meteorol. Soc.*, **96**, 1073–1078,
595 https://doi.org/10.1175/BAMS-D-14-00219.1.

596 Otkin, J. A., and Coauthors, 2016: Assessing the evolution of soil moisture and vegetation
597 conditions during the 2012 United States flash drought. *Agric. For. Meteorol.*, **218**–**219**, 230–
598 242, https://doi.org/10.1016/j.agrformet.2015.12.065.

599 Otkin, J. A., T. Haigh, A. Mucia, M. C. Anderson, and C. Hain, 2018a: Comparison of agricultural
600 stakeholder survey results and drought monitoring datasets during the 2016 u.S. northern
601 plains flash drought. *Weather. Clim. Soc.*, **10**, 867–883, https://doi.org/10.1175/WCAS-D-
602 18-0051.1.

603 ——, M. Svoboda, E. D. Hunt, T. W. Ford, M. C. Anderson, C. Hain, and J. B. Basara, 2018b:
604 Flash Droughts: A Review and Assessment of the Challenges Imposed by Rapid-Onset
605 Droughts in the United States. *Bull. Am. Meteorol. Soc.*, **99**, 911–919,
606 https://doi.org/10.1175/BAMS-D-17-0149.1.

607 Otkin, J. A., and Coauthors, 2021: Development of a Flash Drought Intensity Index.
608 https://doi.org/10.3390/atmos12060741.

609 Peters, A., E. Walter-Shea, L. Ji, A. Viña, M. Hayes, and M. Svoboda, 2002: Drought Monitoring
610 with NDVI-Based Standardized Vegetation Index. *Photogramm. Eng. Remote Sensing*, **68**,
611 71–75.

612 Rouse, J. W. . J., R. H. Haas, J. A. Schell, D. W. Deering, J. W. . J. Rouse, R. H. Haas, J. A. Schell,
613 and D. W. Deering, 1974: Monitoring Vegetation Systems in the Great Plains with Erts.
614 *NASSP*, **351**, 309.

615 Svoboda, M., and Coauthors, 2002: The Drought Monitor. *Bull. Am. Meteorol. Soc.*, **83**, 1181–
616 1190, https://doi.org/10.1175/1520-0477-83.8.1181.

Thorndike, R. L., 1953: Who belongs in the family? *Psychometrika*, **18**, 267–276, https://doi.org/10.1007/BF02289263.

Tian, D., E. F. Wood, and X. Yuan, 2017: CFSv2-based sub-seasonal precipitation and temperature forecast skill over the contiguous United States. *Hydrol. Earth Syst. Sci*, **21**, 1477–1490, https://doi.org/10.5194/hess-21-1477-2017.

Tobin, K. J., W. T. Crow, J. Dong, and M. E. Bennett, 2019: Validation of a New Root-Zone Soil Moisture Product: Soil MERGE. *IEEE J. Sel. Top. Appl. Earth Obs. Remote Sens.*, **12**, 3351–3365, https://doi.org/10.1109/JSTARS.2019.2930946.

Wang, L., X. Yuan, Z. Xie, P. Wu, and Y. Li, 2016: Increasing flash droughts over China during the recent global warming hiatus. *Sci. Rep.*, **6**, https://doi.org/10.1038/srep30571.

Wolf, S., and Coauthors, 2016: Warm spring reduced carbon cycle impact of the 2012 US summer drought. *Proc. Natl. Acad. Sci. U. S. A.*, **113**, 5880–5885, https://doi.org/10.1073/pnas.1519620113.

Yuan, X., L. Wang, P. Wu, P. Ji, J. Sheffield, and M. Zhang, 2019: Anthropogenic shift towards higher risk of flash drought over China. *Nat. Commun.*, **10**, 1–8, https://doi.org/10.1038/s41467-019-12692-7.

Zhang, M., and X. Yuan, 2020: Rapid reduction in ecosystem productivity caused by flash drought based on decade-long FLUXNET observations. *Hydrol. Earth Syst. Sci. Discuss.*, 1–39, https://doi.org/10.5194/hess-2020-185.

Tables:

Table 1: SMVI-NASS and SMVI-NDVI summary hit-miss statistics for the 2012 central region flash drought showing the geographically dominant crops and observed soil moisture conditions.

	Corn	*Range*	*Soybean*	*Sub-soil*	*Topsoil*	*Av. Crop Cond*	*NDVI*
ACC	0.74	0.74	0.78	0.84	0.77	0.75	0.68
CSI	0.71	0.73	0.76	0.84	0.76	0.73	0.63
FDR	0.21	0.07	0.16	0.05	0.05	0.11	0.26
FNR	0.12	0.22	0.10	0.13	0.21	0.20	0.19
FPR	0.65	0.55	0.64	0.50	0.38	0.51	0.60
PPV	0.79	0.93	0.84	0.95	0.95	0.89	0.74
TNR	0.35	0.45	0.36	0.50	0.62	0.49	0.40
TPR	0.88	0.78	0.90	0.87	0.79	0.80	0.81

Table 2: As in Table 1, but for the 2017 northern high plains region flash drought.

	Barley	*Oats*	*Spring Wheat*	*Winter Wheat*	*Sub-soil*	*Topsoil*	*Av. Crop Cond*	*NDVI*
ACC	0.80	0.73	0.76	0.78	0.84	0.84	0.72	0.56
CSI	0.79	0.72	0.75	0.77	0.83	0.83	0.70	0.48
FDR	0.09	0.15	0.12	0.08	0.03	0.02	0.18	0.50
FNR	0.15	0.18	0.16	0.17	0.15	0.16	0.17	0.07

FPR	0.55	0.73	0.65	0.61	0.29	0.25	0.72	0.72
PPV	0.91	0.85	0.88	0.92	0.97	0.98	0.82	0.50
TNR	0.45	0.27	0.35	0.39	0.71	0.75	0.28	0.28
TPR	0.85	0.82	0.84	0.83	0.85	0.84	0.83	0.93

642

Figures:

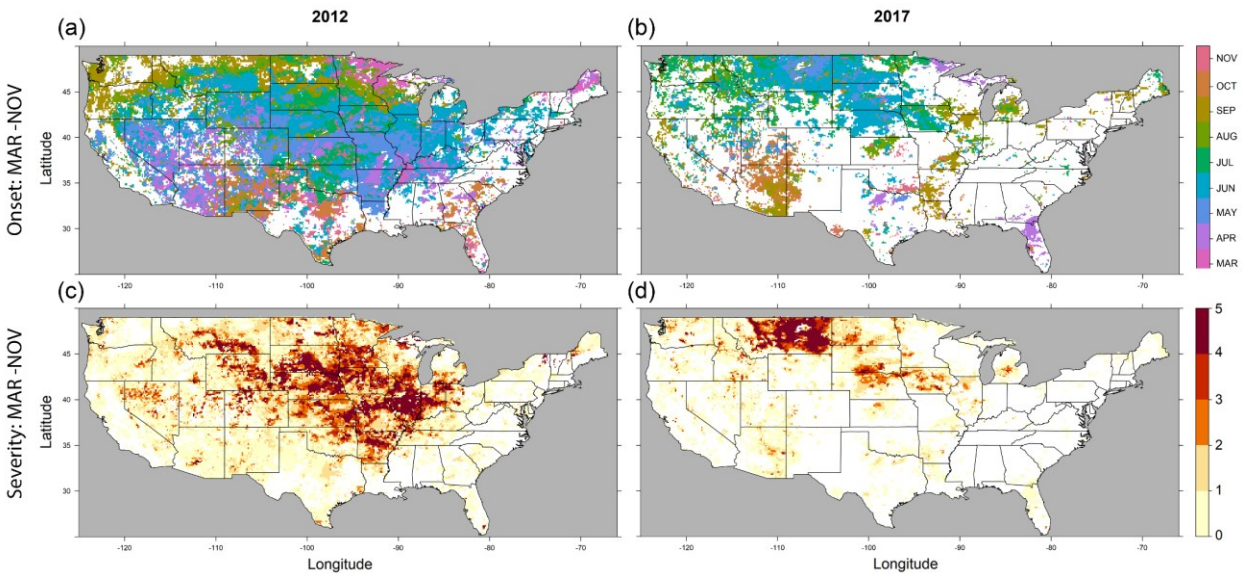

Figure 1: Flash drought maps as captured by SMVI definition during the active growing season (Mar-Nov). left column for 2012 and the right column for 2017. Panels (a) and (b): Onset maps where each color represents the month of flash drought onset. Bottom row: Estimated severity category maps.

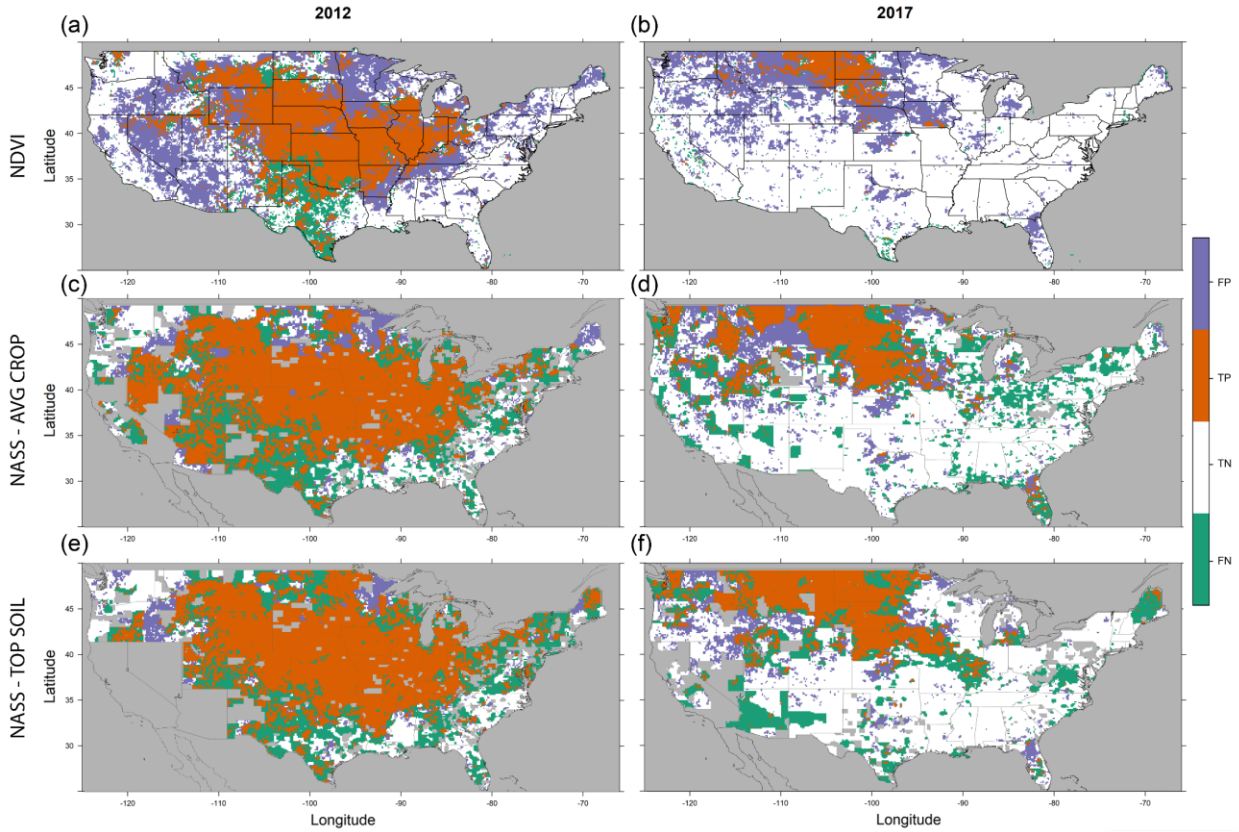

649

650 *Figure 2: Maps of hit-miss analysis for the 2012 and the 2017 flash droughts during the actively*
651 *growing season (Mar-Nov). Left column for 2012 and right column for 2017. Panels (a) and (b):*
652 *SMVI vs. negative NDVI anomaly hit-miss map, in which lavender represents False Positive (FP),*
653 *orange represents True Positive (TP), white represents True Negative (TN), green represents*
654 *False Negative (FN), and grey represents missing/unavailable data. Panels (c) and (d): similar to*
655 *(a) and (b)for NASS reported negative average crop conditions. Panels (e) and (f): similar to (a)*
656 *and (b)for the observed topsoil moisture.*

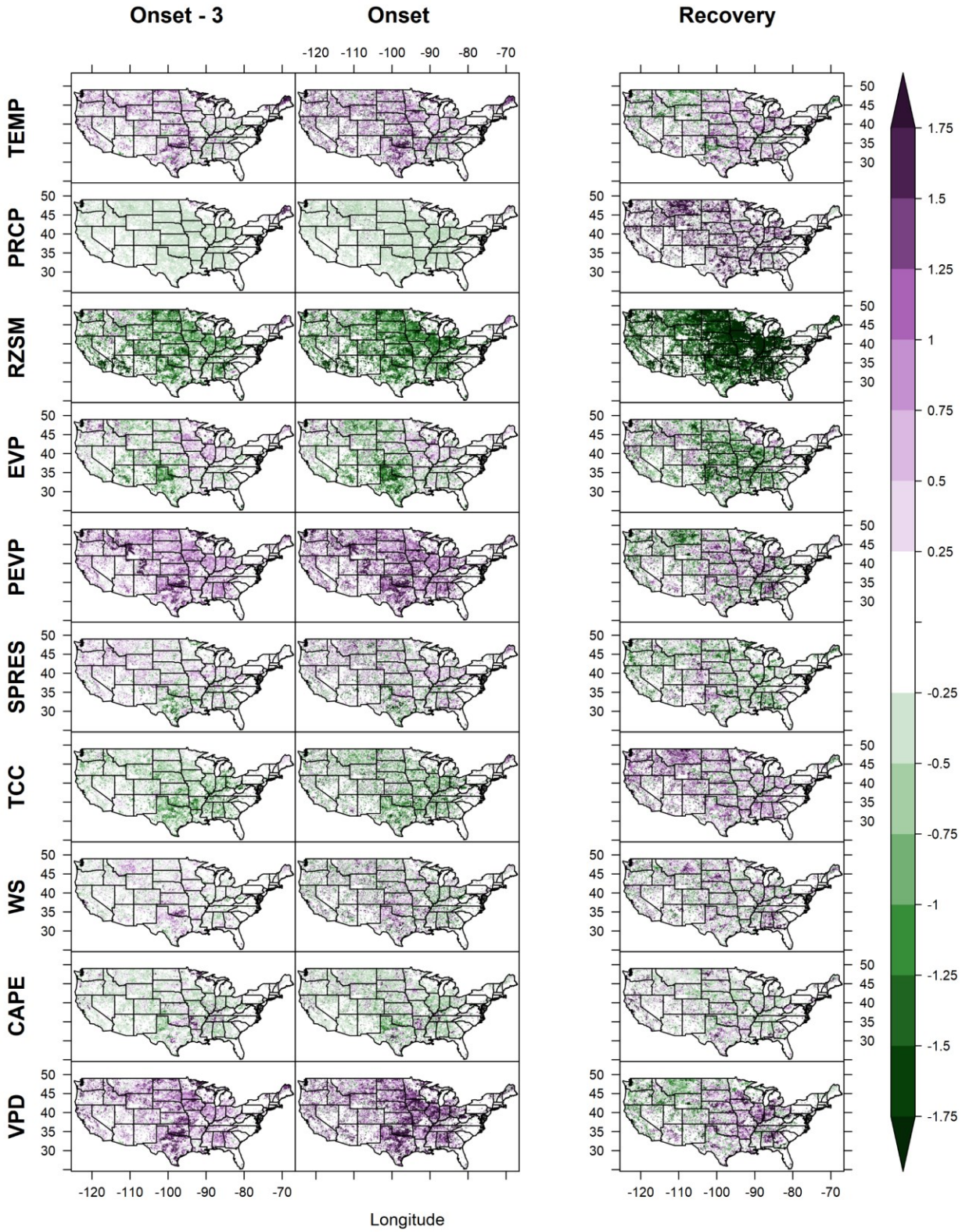
Onset - 3
Onset
Recovery
TEMP
PRCP
RZSM
EVP
PEVP
SPRES
TCC
WS
CAPE
VPD
-120 -110 -100 -90 -80 -70
50 45 40 35 30
1.75
1.5
1.25
1
0.75
0.5
0.25
-0.25
-0.5
-0.75
-1
-1.25
-1.5
-1.75
Longitude

657

Figure 3: Composite maps of standardized anomalies of climate conditions for selected atmospheric variables (TEMP: 2-m above ground Temperature, PRCP: Precipitation, RZSM: Root-zone soil moisture, EVP: Actual evapotranspiration, PEVP: Potential evapotranspiration, SPRESS: Surface pressure, TCC: Total cloud cover, WS: 10-m above ground wind speed and CAPE: Convective Available Potential Energy, VPD = Vapor Pressure Deficit) based on the full SMVI flash droughts inventory from 1979-2018 for severity higher than '2', during onset, recovery, and onset minus 3 pentads.

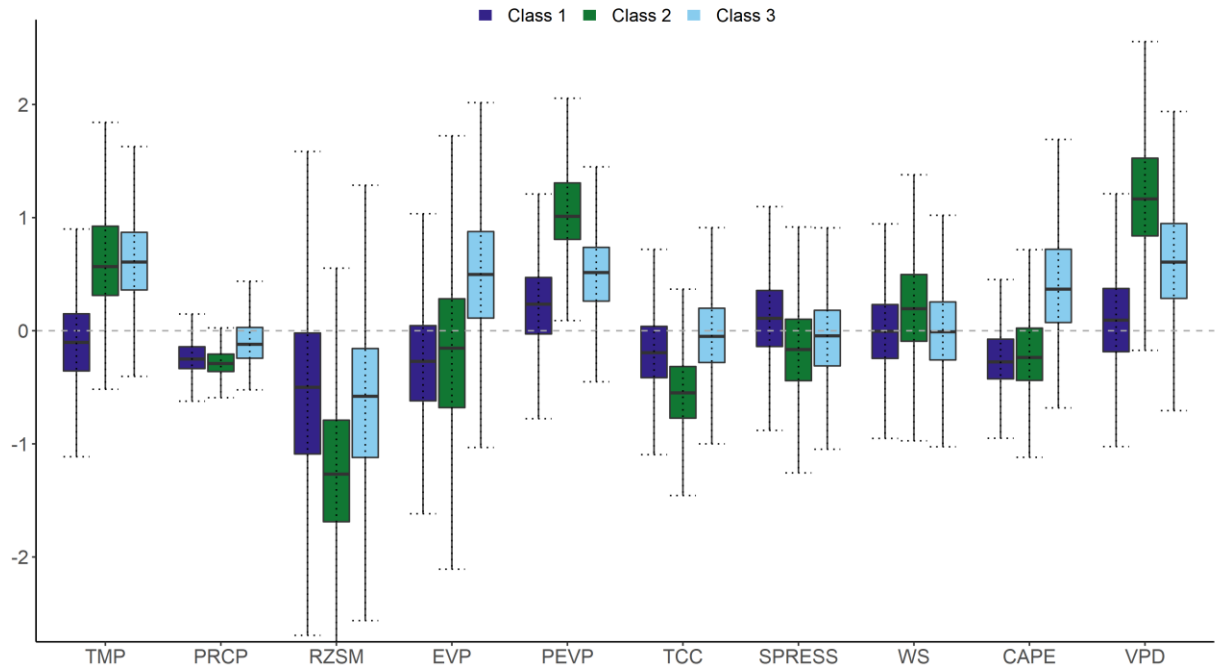

Figure 4: Box plot of the standardized anomalies of atmospheric variables and root zone soil moisture averaged for the three pentads before drought onset for each Class for the full SMVI inventory from 1979 to 2018. A separate figure for each of the fields' variability across years is

shown in Figure S4. Maps of the anomalies averaged over the three pentads prior to onset are shown in Figure S5.

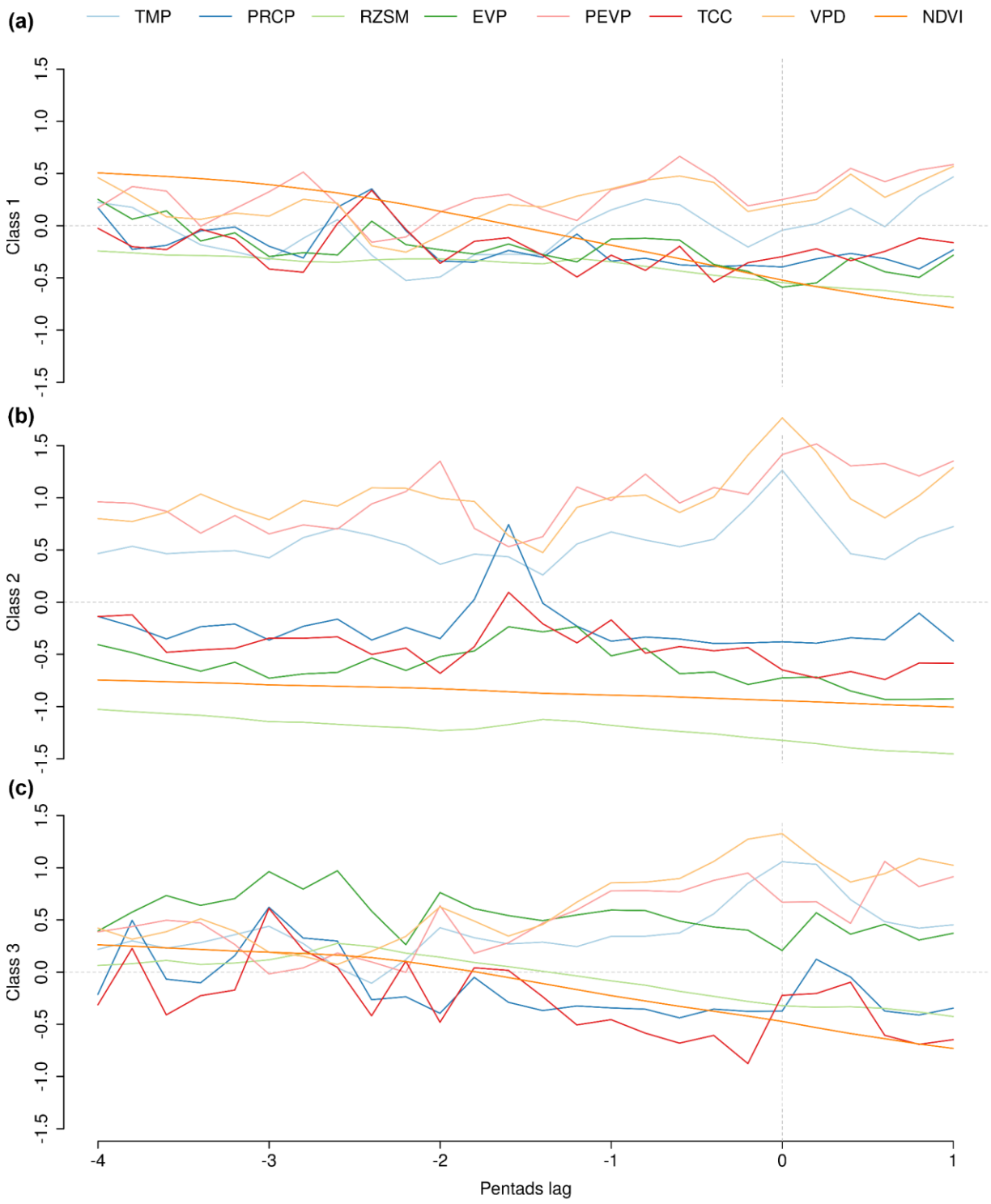

673

674 *Figure 5: Daily time series plots of selected atmospheric variables and RZSM from four pentads*

675 *prior to drought onset to one pentad after onset for (a) Class 1, (b) Class 2, and (c) Class 3 events.*

676 *For each class, the time series of each variable represents an average of 20 grid cells, each*
677 *selected from the core area of a separate flash drought event. The Y-axis shows the standard*
678 *deviation for the normalized variables' values.*

679

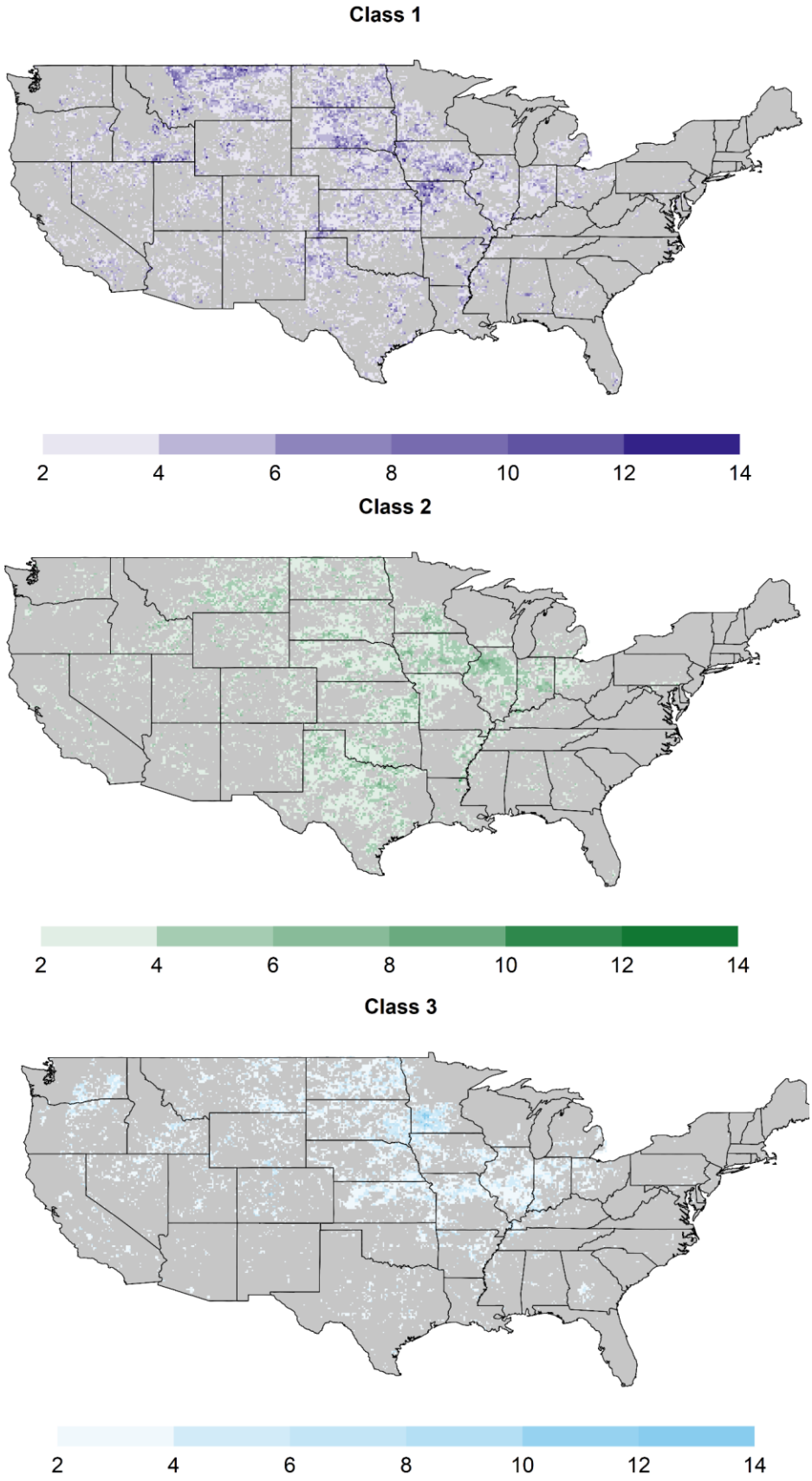

680

Figure 6: Frequency (% of years with an event) for each flash drought class at each grid point for the period 1979 to 2018, based on the SMVI flash droughts definition.

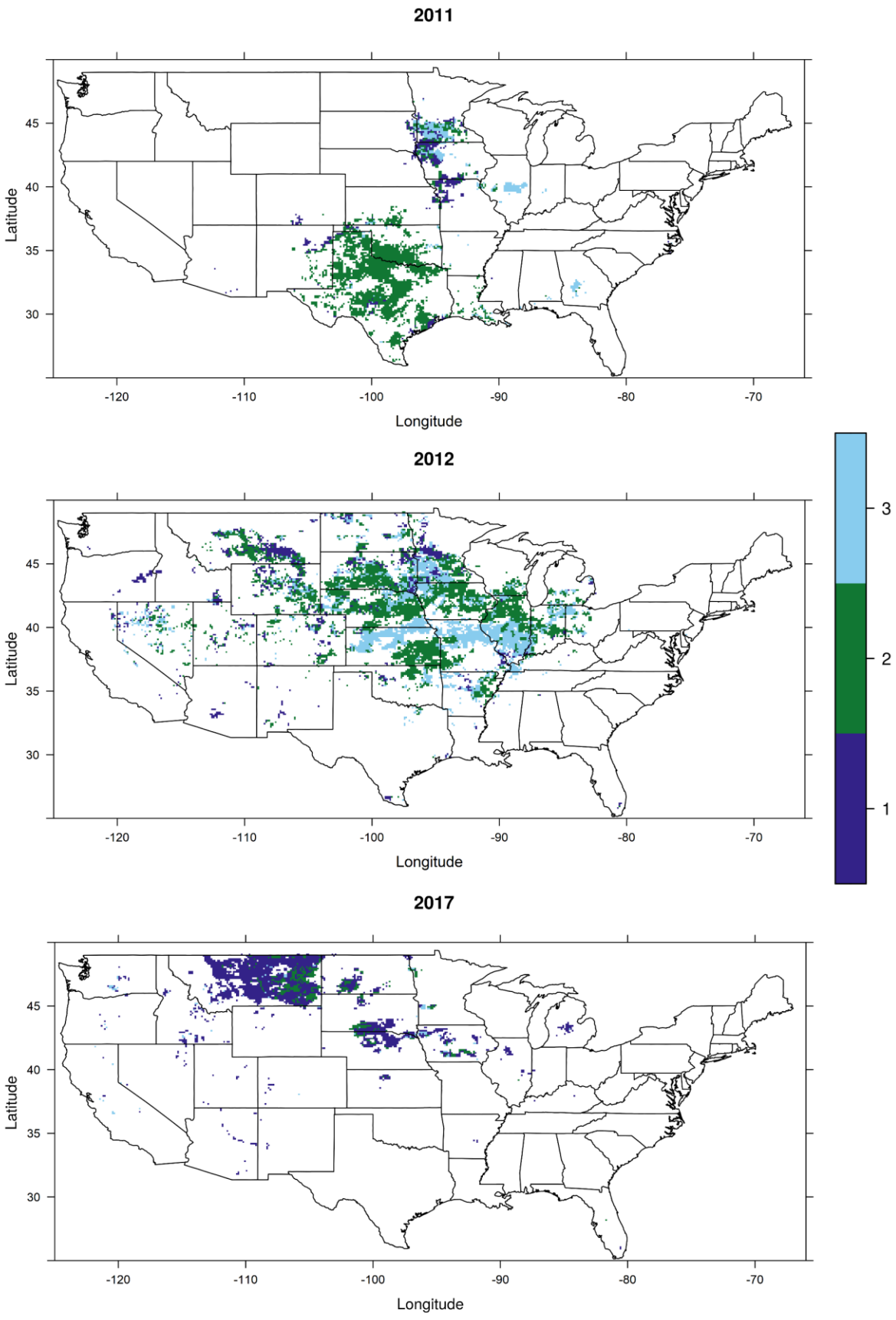
2011
2012
2017
Latitude
Longitude
45
40
35
30
-120
-110
-100
-90
-80
-70
3
2
1

683

684 *Figure 7: Classification maps of the 2011, 2012 and 2017 flash drought events.*

685

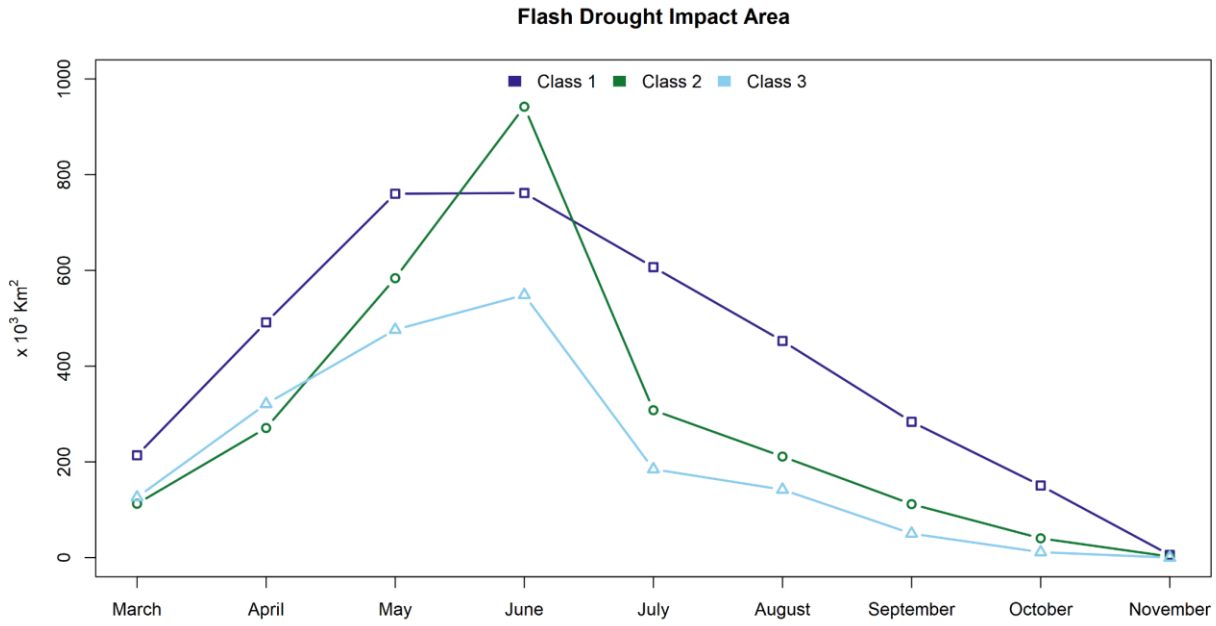

686

687 *Figure 8: Average area in each flash drought class in each month included in this study. Average*

688 *is calculated for the 1979-2018 period.*

689

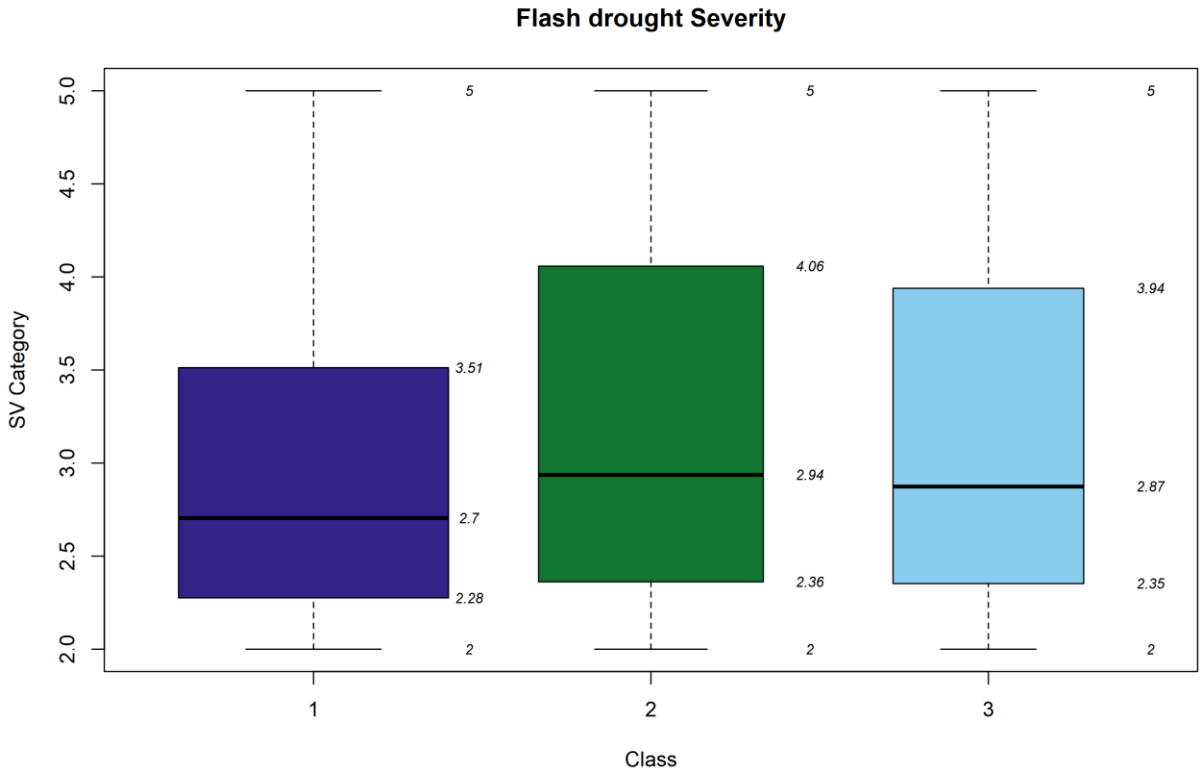

690

691 *Figure 9: Box plots of the flash droughts average severity categories in the three classes after*
692 *filtering out events of severity category less than 2 (box widths are proportional to the square root*
693 *of the total number of grid-points in each class).*